

Ironing out primordial temperature fluctuations with polarization: optimal detection of cosmic structure imprints

M. Frommert[★] and T. A. Enßlin

Max-Planck-Institut für Astrophysik, Karl-Schwarzschild-Straße 1, D-85748 Garching b. München, Germany

Accepted 2009 February 12. Received 2009 January 28; in original form 2008 November 26

ABSTRACT

Secondary anisotropies of the cosmic microwave background (CMB) can be detected by using the cross-correlation between the large-scale structure (LSS) and the CMB temperature fluctuations. In such studies, chance correlations of primordial CMB fluctuations with the LSS are the main source of uncertainty. We present a method for reducing this noise by exploiting information contained in the polarization of CMB photons. The method is described in general terms and then applied to our recently proposed optimal method for measuring the integrated Sachs–Wolfe (ISW) effect. We obtain an expected signal-to-noise ratio of up to 8.5. This corresponds to an enhancement of the signal-to-noise ratio by 23 per cent as compared to the standard method for ISW detection, and by 16 per cent w.r.t. our recently proposed method, both for the best-case scenario of having perfect (noiseless) CMB and LSS data.

Key words: cosmic microwave background – large-scale structure of Universe.

1 INTRODUCTION

The low-redshift large-scale structure (LSS) changes the cosmic microwave background (CMB) fluctuations in various ways. Such secondary effects on the CMB are, for example, the integrated Sachs–Wolfe (ISW) effect (Sachs & Wolfe 1967), the Rees–Sciama (RS) effect (Rees & Sciama 1968), gravitational lensing (Lewis & Challinor 2006) and the Sunyaev–Zel’dovich (SZ) effect (Sunyaev & Zeldovich 1972, 1980). By studying these signals, we can obtain valuable information about our Universe. The ISW effect, for example, provides independent evidence for the existence of dark energy. Unfortunately, unless the spectral signatures of the signal differ from the ones of the primordial CMB, it is difficult to detect them. The reason is that the primordial CMB fluctuations created at the time of last scattering are much stronger than the secondary temperature anisotropies. The usual method for detecting secondary anisotropies in the CMB is via cross-correlating the CMB temperature maps with LSS data such as the galaxy density contrast. Since secondary anisotropies in the CMB are created by the LSS, there is a significant cross-correlation between the two. In contrast, the primordial CMB fluctuations should not be correlated with the LSS. By performing the cross-correlation analysis, one can therefore separate signatures of the presence of these secondary anisotropies from the primordial fluctuations.

In the standard cross-correlation method, first described by Boughn, Crittenden & Turok (1998), the observed cross-correlation between LSS and CMB data is compared to its theoretical prediction. This method has been extensively used to detect the ISW effect. Some of the most recent studies are by Ho et al. (2008),

Giannantonio et al. (2008), Rassat et al. (2006) and Boughn & Crittenden (2004). Since the theoretical cross-correlation function is by construction an ensemble average over all possible universes, fluctuations associated with the specific realization of the LSS in the observed Universe act as a source of noise in the detected signal in the standard method.

In Frommert, Enßlin & Kitaura (2008), we suggested a method for reducing this source of uncertainty, which we will refer to as the optimal temperature-only method. Instead of comparing the observed cross-correlation function with its theoretical prediction, we use an optimal matched filter in order to detect an ISW template in CMB data. Similar schemes were independently proposed by Zhang (2006), Hernández-Monteagudo (2008) and Granett, Neyrinck & Szapudi (2008). Optimal matched filters have also been used to study other secondary effects on the CMB. The first of these studies explored the detectability of the kinetic SZ effect of galaxy clusters (Haehnelt & Tegmark 1996), later works on the kinetic SZ and the RS effects are for example by Schäfer et al. (2006), Maturi et al. (2007a,b) and Waelkens, Maturi & Enßlin (2008).

However, in both the standard method and the optimal temperature-only method, the main source of uncertainty in the detection of the secondary signal comes from chance correlations of primordial CMB fluctuations with the LSS. In this work, we present a method which exploits polarization information in order to reduce not only the noise from the specific LSS realization but also the noise coming from primordial CMB temperature fluctuations. This method can be applied generically to the detection of all secondary effects. It is based on the fact that the polarization measured in the CMB contains information about the primordial temperature fluctuations. We use the observed E-mode polarization map, which we translate into a temperature map using the temperature-E-mode cross-power spectrum. The obtained

[★]E-mail: mona@mpa-garching.mpg.de

temperature map is then subtracted from the observed temperature map, and hence no longer contributes to the noise budget of the detected signal. Once an E map has been measured to a good accuracy, this will significantly enhance the signal-to-noise ratio (S/N) of the detection of secondary effects. The first all-sky measurement of polarization with high fidelity is expected to be provided by the Planck Surveyor satellite (Tauber 2000), to be launched in 2009.

Our optimal polarization method builds on the optimal scheme to detect LSS signatures in CMB data, which we developed in Frommert et al. (2008) specifically for the ISW effect. Note that this method assumes a Gaussian data model, hence it is very well suited for the ISW effect, whereas one might need to extend it into the non-Gaussian regime for other effects such as the RS effect, the kinetic SZ effect or lensing. This can be done using information field theory (Enßlin, Frommert & Kitaura 2008), but is beyond the scope of this work. Here, we show how to use the information contained in polarization data within the framework of a Gaussian data model and leave the extension to more complicated models for future work.

When applying our method to ISW detection, we obtain an expected S/N of up to 8.5. This corresponds to an enhancement of the S/N by 16 per cent w.r.t. the optimal temperature-only method, independent of the depth of the galaxy survey considered. In comparison to the standard method, the S/N is enhanced by 23 per cent for a full-sky LSS survey that goes out to redshift 2. Both of these comparisons have been made for the best-case scenario of having perfect (noiseless) CMB and LSS data.

Using polarization data to reduce the noise in the detection of secondary effects was first proposed by Robert Crittenden, following a suggestion from Lyman Page (Crittenden 2006). He already derived the reduced temperature power spectrum, which we show in Fig. 1, and roughly estimates the improvement of the S/N for ISW detection to be around 20 per cent, which we confirm with our calculations.

Our article is organized as follows. In Section 2, we describe the optimal method derived in Frommert et al. (2008) in general terms. In Section 3, we then show how we can reduce the noise coming from primordial temperature fluctuations by using polarization data. In Section 4, we apply the method to the ISW effect. We conclude in Section 5.

2 OPTIMAL METHOD FOR THE DETECTION OF SECONDARY EFFECTS ON THE CMB

In Frommert et al. (2008), we derived an optimal method for the detection of secondary temperature anisotropies in the CMB using as example the ISW effect. In this section, we briefly review this method, which we refer to as the optimal temperature-only method.

Let us assume that we know the LSS well enough to create a template T_τ of the secondary signal T_s that we would like to detect in the temperature fluctuations, for example, the ISW signal T_{isw} . Here, T_X with any index X denotes the function $T_X : S^2 \rightarrow \mathbb{R}$, which we regard also as an element of a function vector space. The data d we measure are the observed CMB temperature fluctuations T_{obs} . Our data model is then

$$\begin{aligned} d &\equiv T_{\text{obs}} \\ &= T_{\text{cmb}} + T_{\text{fg}} + T_{\text{det}} \\ &= T_\tau + (T_{\text{cmb}} - T_\tau) + T_{\text{fg}} + T_{\text{det}} \\ &\equiv T_\tau + \Delta T_{\text{obs}}, \end{aligned} \quad (1)$$

where T_{cmb} denotes the cosmological CMB temperature fluctuations, T_{fg} are residual galactic foregrounds after foreground removal and T_{det} denotes the detector noise. Note that $(T_{\text{cmb}} - T_\tau) = (T_{\text{cmb}} - T_s) + (T_s - T_\tau)$ contains the CMB fluctuations other than the signal we are after, $(T_{\text{cmb}} - T_s)$, and the uncertainty in the template w.r.t. the signal, $(T_s - T_\tau)$, coming from our ignorance of the full distribution of the matter in the Universe. Note that for simplifying the notation we have redefined $T \equiv (T - T_0)/T_0$, where T_0 denotes the monopole of the CMB temperature fluctuations. An overview over the above definitions can be found in Table 1.

We now approximate the distribution of ΔT_{obs} by a Gaussian around zero. That is, we write the probability density function of T_{obs} given the signal template T_τ and the cosmological parameters p , the likelihood, as

$$P(T_{\text{obs}} | T_\tau, p) = \mathcal{G}(T_{\text{obs}} - T_\tau, \mathbf{C}). \quad (2)$$

Here, we have defined

$$\mathcal{G}(\chi, \mathbf{C}) \equiv \frac{1}{\sqrt{|2\pi\mathbf{C}|}} \exp\left(-\frac{1}{2}\chi^\dagger \mathbf{C}^{-1} \chi\right) \quad (3)$$

to denote the probability density function of a Gaussian-distributed vector χ with zero mean, given the cosmological parameters p and the covariance matrix $\mathbf{C} \equiv \langle \chi \chi^\dagger \rangle$, where the averages are taken over the Gaussian distribution $\mathcal{G}(\chi, \mathbf{C})$. Note that in general the covariance matrix depends on the cosmological parameters, which is not explicitly stated in our notation. A daggered vector or matrix denotes its transposed and complex conjugated version, as usual. Hence, given two vectors a and b , ab^\dagger must be read as the tensor product, whereas $a^\dagger b$ denotes the scalar product. Note that in equation (2) the signal template T_τ may depend on the cosmological parameters p as well.

Let us briefly address the question of how to create the template T_τ . When writing down the likelihood in equation (2), we have implicitly assumed that the template T_τ is the mean of T_{obs} w.r.t. the probability distribution given in equation (2). This probability distribution is conditional on the template T_τ , or, in other words, conditional on the LSS data δ_g , from which we have created our template according to some prescription. Note that usually δ_g denotes the galaxy density contrast, but we use it to denote the LSS data in a more general sense here, which could also be lensing information for example.

In the following, we assume that the signal $T_s = R \delta_m$ is given by a linear operator R applied to the matter density contrast δ_m . For the ISW effect, the operator R is explicitly derived in Frommert et al.

Table 1. Summary of defined symbols.

Symbol	Definition
$T_{\text{cmb}}, E_{\text{cmb}}$	Cosmological CMB temperature and polarization
T_s, E_s	Real secondary signal that we are trying to detect
T_τ, E_τ	Signal templates for temperature and polarization
$T_{\text{fg}}, E_{\text{fg}}$	Residual galactic foregrounds after foreground removal
$T_{\text{det}}, E_{\text{det}}$	Detector noise
$T_{\text{obs}}, E_{\text{obs}}$	$(T_{\text{cmb}} + T_{\text{fg}} + T_{\text{det}}), (E_{\text{cmb}} + E_{\text{fg}} + E_{\text{det}})$
$\Delta T_{\text{obs}}, \Delta E_{\text{obs}}$	$(T_{\text{obs}} - T_\tau), (E_{\text{obs}} - E_\tau)$
T_{isw}	Fluctuations created by ISW effect
T_{prim}	$(T_{\text{cmb}} - T_{\text{isw}})$

(2008). We can then write

$$\begin{aligned}
 T_\tau &\equiv \langle T_{\text{obs}} \rangle_{P(T_{\text{obs}} | \delta_{g,p})} \\
 &\approx \langle T_s \rangle_{P(T_s | \delta_{g,p})} + \langle (T_{\text{cmb}} - T_s) \rangle_{P[(T_{\text{cmb}} - T_s) | \delta_{g,p}]} \\
 &\quad + \langle T_{\text{fg}} \rangle_{P(T_{\text{fg}} | \delta_{g,p})} + \langle T_{\text{det}} \rangle_{P(T_{\text{det}})} \\
 &= R \langle \delta_m \rangle_{P(\delta_m | \delta_{g,p})}, \tag{4}
 \end{aligned}$$

where we have used that T_s , $(T_{\text{cmb}} - T_s)$, T_{fg} and T_{det} are approximately stochastically independent in the first step and that the three errors have vanishing means, $\langle (T_{\text{cmb}} - T_s) \rangle_{P[(T_{\text{cmb}} - T_s) | \delta_{g,p}]} = \langle T_{\text{fg}} \rangle_{P(T_{\text{fg}} | \delta_{g,p})} = \langle T_{\text{det}} \rangle_{P(T_{\text{det}})} = 0$, in the second step. For the ISW effect, $(T_{\text{cmb}} - T_s) \equiv (T_{\text{cmb}} - T_{\text{isw}}) = T_{\text{prim}}$ are simply the primordial fluctuations, which do have zero mean (Frommert et al. 2008). For other secondary effects, $\langle (T_{\text{cmb}} - T_s) \rangle_{P[(T_{\text{cmb}} - T_s) | \delta_{g,p}]} = 0$ is probably still a reasonably good approximation. In the last step, we have pulled the operator R out of the mean.

We see that for creating the signal template T_τ we need the mean of the matter density contrast conditional on the LSS data, $\langle \delta_m \rangle_{P(\delta_m | \delta_{g,p})}$. In the simplest case of having a Gaussian likelihood and Gaussian prior for δ_m , this is given by the Wiener filter. Again this is a very good approximation for the ISW effect, which is present on very large scales, on which structure growth is still linear. For other effects such as the kinetic SZ effect, the RS effect or lensing, the Gaussian approximation for δ_m may not be very good (thus also the Gaussian approximation for ΔT_{obs} may not be good), and one would have to consider non-Gaussian data models using information field theory (Enßlin et al. 2008). However, in this work we will use the Gaussian data model and leave extensions to non-Gaussian models for future work. Note that, when choosing the template as in equation (4), the latter is uncorrelated with $\Delta T_{\text{obs}} \equiv (T_{\text{obs}} - T_\tau)$ (w.r.t. the probability distribution in equation 2), as can be easily shown.

In order to see how well we can recover such a signal template from the CMB data, we put an amplitude A_τ in front of the signal T_τ in equation (2), and try to estimate its value from the data (the true value of this amplitude is 1, of course):

$$P(T_{\text{obs}} | A_\tau, T_\tau, p) = \mathcal{G}(T_{\text{obs}} - A_\tau T_\tau, \mathbf{C}). \tag{5}$$

The maximum likelihood estimator \hat{A}_τ for the amplitude A_τ is

$$\hat{A}_\tau = \frac{T_{\text{obs}}^\dagger \mathbf{C}^{-1} T_\tau}{T_\tau^\dagger \mathbf{C}^{-1} T_\tau} = \frac{\sum_l (2l+1) \frac{\hat{C}_l^{T_\tau, T_{\text{obs}}}}{C_l^{\Delta T_{\text{obs}}}}}{\sum_l (2l+1) \frac{\hat{C}_l^{T_\tau}}{C_l^{\Delta T_{\text{obs}}}}}. \tag{6}$$

In the second equality, we have assumed that the knowledge of the secondary anisotropy template is equally good in any direction, so that the template uncertainty matrix is isotropic and fully described by its spherical harmonics power spectrum. We will use this assumption also in the following. This permits us to evaluate the expressions in spherical harmonics space in the second step. We have used the following definitions of the power spectra and their estimators (we use a hat to denote estimators)

$$C_l^{X,Y} \equiv \langle a_{lm}^X a_{lm}^{Y*} \rangle, \tag{7}$$

$$C_l^X \equiv C_l^{X,X}, \tag{8}$$

$$\hat{C}_l^{X,Y} \equiv \frac{1}{2l+1} \sum_l \text{Re} \left(\hat{a}_{lm}^X \hat{a}_{lm}^{Y*} \right), \tag{9}$$

$$\hat{C}_l^X \equiv \hat{C}_l^{X,X}, \tag{10}$$

where the a_{lm} are defined by an expansion into spherical harmonics Y_{lm} :

$$a_{lm}^X \equiv \int_S d\Omega T_X(\hat{\mathbf{n}}) Y_{lm}^*(\hat{\mathbf{n}}). \tag{11}$$

The power spectrum $C_l^{\Delta T_{\text{obs}}}$ denotes the spherical harmonics space version of the covariance matrix \mathbf{C} . We calculate the variance of the amplitude estimator to be

$$\begin{aligned}
 \sigma_A^2 &\equiv \left\langle \left(\hat{A}_\tau - \langle \hat{A}_\tau \rangle_{\text{cond}} \right)^2 \right\rangle_{\text{cond}} \\
 &= \left(T_\tau^\dagger \mathbf{C}^{-1} T_\tau \right)^{-1} = \left[\sum_l (2l+1) \frac{\hat{C}_l^{T_\tau}}{C_l^{\Delta T_{\text{obs}}}} \right]^{-1}, \tag{12}
 \end{aligned}$$

where we have again evaluated the expressions in spherical harmonics space in the last step, and we have used the notation introduced in Frommert et al. (2008), where the index ‘cond’ indicates that the average is taken conditional on the signal template T_τ , i.e. over the probability distribution given in equation (2). We can now define the S/N as follows

$$\left(\frac{S}{N} \right)_t \equiv \frac{1}{\sigma_A^2} = \sum_l (2l+1) \frac{\hat{C}_l^{T_\tau}}{C_l^{\Delta T_{\text{obs}}}}, \tag{13}$$

where the index t indicates that this is the S/N one obtains for the optimal temperature-only method. This S/N depends on the actual realization of the matter distribution in our Universe via the estimator $\hat{C}_l^{T_\tau}$. In Frommert et al. (2008), we showed that for the ISW effect we obtain on average a S/N of about 7, if we assume an ideal LSS survey which covers the whole sky and goes out to a redshift of about 2. In comparison to the standard method, this is an enhancement of the S/N by about 7 per cent.

3 REDUCTION OF THE PRIMORDIAL NOISE USING POLARIZATION INFORMATION

With the method suggested in Frommert et al. (2008), we were able to reduce the low-redshift cosmic variance effect in amplitude estimates of secondary signals, i.e. we reduced the noise coming from the specific realization of LSS in our Universe. Now, we show how even the noise coming from primordial temperature fluctuations can be reduced. The idea is that since the temperature and polarization maps of the CMB are correlated, the polarization contains information about the temperature fluctuations. After extracting this information from the polarization data, we know a part of the temperature map, which we can remove from the data before trying to detect the signal. In other words, we make our amplitude estimate of the secondary signal conditional on the known part of the temperature fluctuations.

To include the information contained in the polarization data, we enlarge our data vector d to include the observed E-mode polarization map E_{obs} as well:

$$d \equiv (T_{\text{obs}}, E_{\text{obs}})^t, \tag{14}$$

or, in spherical harmonics space

$$a_{lm}^d \equiv \left(a_{lm}^{T_{\text{obs}}}, a_{lm}^{E_{\text{obs}}} \right)^t. \tag{15}$$

Note that with *the map* E_{obs} , we are referring again to the abstract element of a function vector space, which contains all the information on the observed E mode. When evaluating the abstract expressions obtained in the following, we use the representation of E_{obs} in spherical harmonics space, consisting of all coefficients $a_{lm}^{E_{\text{obs}}}$.

In principle, it is possible that the secondary effect we are looking for is also present as a small signal in the polarization data. If the temperature anisotropies created by the secondary effect exhibit a quadrupole component at the time of reionization, this quadrupole will be rescattered by free electrons and create a polarization signal (Zaldarriaga 1997). However, for the ISW this effect has been proven to be small (Cooray & Melchiorri 2006). It should also be small for the RS effect, lensing and the kinetic SZ effect, the highest contributions of which are on relatively small scales. Thus, as a first approximation we assume that the polarization data do not carry any signal of the effect we want to detect. Our signal template τ is then

$$\begin{aligned}\tau &\equiv (T_\tau, 0)^t, \\ a_{lm}^\tau &\equiv (a_{lm}^{T_\tau}, 0)^t,\end{aligned}\quad (16)$$

and the data model becomes

$$d = \begin{pmatrix} T_{\text{obs}} \\ E_{\text{obs}} \end{pmatrix} = \begin{pmatrix} T_\tau + \Delta T_{\text{obs}} \\ E_{\text{obs}} \end{pmatrix}.\quad (17)$$

The observed E map, $E_{\text{obs}} = E_{\text{cmb}} + E_{\text{fg}} + E_{\text{det}}$, consists of the cosmological E-mode fluctuations E_{cmb} , residual galactic foregrounds after foreground removal E_{fg} and the detector noise E_{det} . Assuming again Gaussianity, we can write down the likelihood

$$P(d | \tau, p) = \mathcal{G}(d - \tau, \tilde{\mathbf{C}}),\quad (18)$$

where the covariance matrix $\tilde{\mathbf{C}}$ is

$$\tilde{\mathbf{C}} \equiv \langle (d - \tau)(d - \tau)^\dagger \rangle_{\text{cond}},\quad (19)$$

and we have redefined the index ‘cond’ to denote the average over the probability distribution in equation (18). In spherical harmonics space, the covariance matrix $\tilde{\mathbf{C}}$ is block diagonal with the blocks being

$$\tilde{\mathbf{C}}(l) = \begin{pmatrix} C_l^{\Delta T_{\text{obs}}} & C_l^{\Delta T_{\text{obs}}, E_{\text{obs}}} \\ C_l^{\Delta T_{\text{obs}}, E_{\text{obs}}} & C_l^{E_{\text{obs}}} \end{pmatrix}.\quad (20)$$

Therefore, the likelihood factorizes:

$$P(d | \tau, p) = \prod_{l,m} \mathcal{G}[a_{lm}^d - a_{lm}^\tau, \tilde{\mathbf{C}}(l)].\quad (21)$$

When inserting the inverse of the covariance matrix $\tilde{\mathbf{C}}(l)$, it is possible to rewrite the likelihood as a product of a reduced temperature part and a polarization part. To this end, let us define the reduced temperature map and power spectrum:

$$\begin{aligned}a_{lm}^{T_{\text{red}}} &\equiv a_{lm}^{T_{\text{obs}}} - \frac{C_l^{\Delta T_{\text{obs}}, E_{\text{obs}}}}{C_l^{E_{\text{obs}}}} a_{lm}^{E_{\text{obs}}}, \\ C_l^{\text{red}} &\equiv C_l^{\Delta T_{\text{obs}}} - \frac{(C_l^{\Delta T_{\text{obs}}, E_{\text{obs}}})^2}{C_l^{E_{\text{obs}}}}.\end{aligned}\quad (22)$$

With these definitions, the likelihood becomes

$$P(d | \tau, p) = \prod_{l,m} \left[\mathcal{G}\left(a_{lm}^{T_{\text{red}}} - a_{lm}^{T_\tau}, C_l^{\text{red}}\right) \mathcal{G}\left(a_{lm}^{E_{\text{obs}}}, C_l^{E_{\text{obs}}}\right) \right],\quad (23)$$

as we prove in Appendix A. Now, our goal is to find the signal template T_τ in the CMB data. The polarization part of the above likelihood, $\mathcal{G}(a_{lm}^{E_{\text{obs}}}, C_l^{E_{\text{obs}}})$, does not depend on the signal template, nor does the reduced temperature part explicitly depend on E_{obs} . In other words, the observed E map does not contain relevant information any more after introducing the reduced temperature fluctuations. Thus, we can marginalize over it, and continue only with the

likelihood of the reduced temperature map

$$\begin{aligned}P(T_{\text{red}} | T_\tau, p) &\equiv \mathcal{G}(T_{\text{red}} - T_\tau, \mathbf{C}_{\text{red}}) \\ &= \prod_{l,m} \mathcal{G}\left(a_{lm}^{T_{\text{red}}} - a_{lm}^{T_\tau}, C_l^{\text{red}}\right).\end{aligned}\quad (24)$$

Note that it is straightforward to derive the factorized likelihood also for the case that we do have a non-zero signal template E_τ for the polarization part. In that case, the covariance matrix $\tilde{\mathbf{C}}(l)$ is slightly changed, as well as the definitions of the reduced temperature map and power spectrum, and we can no longer neglect the polarization part of the likelihood. Please refer to Appendix A for details.

Let us pause for a second and have a closer look at the quantities defined in equation (22). What we have effectively done is the following. We have a polarization map $a_{lm}^{E_{\text{obs}}}$, which is correlated with the temperature fluctuations $a_{lm}^{\Delta T_{\text{obs}}}$ via $C_l^{\Delta T_{\text{obs}}, E_{\text{obs}}}$. That is, the polarization map contains information about the temperature map, which we can translate into a ‘known’ part of the temperature map using the prescription $(C_l^{\Delta T_{\text{obs}}, E_{\text{obs}}} / C_l^{E_{\text{obs}}}) a_{lm}^{E_{\text{obs}}}$. This known part of the temperature map is subtracted from the observed one, and we work only with the remaining unknown temperature fluctuations in which we try to detect our signal template.

The reduced temperature map fluctuates around our signal template T_τ only with the variance C_l^{red} , which is smaller than the full variance $C_l^{\Delta T_{\text{obs}}}$ of the observed temperature map. This reduced variance is the uncertainty going into our signal-detection problem now, rather than the full variance of the original temperature fluctuations.

In order to see this, let us again put an amplitude in front of the signal template in equation (24) and estimate it from the data using a maximum likelihood estimator:

$$\hat{A}_\tau = \frac{T_\tau^\dagger \mathbf{C}_{\text{red}}^{-1} \mathbf{T}_\tau}{T_\tau^\dagger \mathbf{C}_{\text{red}}^{-1} \mathbf{T}_\tau} = \frac{\sum_l (2l+1) \frac{\hat{C}_l^{T_{\text{red}}, T_\tau}}{C_l^{\text{red}}}}{\sum_l (2l+1) \frac{\hat{C}_l^{T_\tau}}{C_l^{\text{red}}}}.\quad (25)$$

Here, the last expression is in spherical harmonics space. The variance of \hat{A}_τ is now

$$\sigma_A^2 = (T_\tau^\dagger \mathbf{C}_{\text{red}}^{-1} \mathbf{T}_\tau)^{-1} = \left[\sum_l (2l+1) \frac{\hat{C}_l^{T_\tau}}{C_l^{\text{red}}} \right]^{-1},\quad (26)$$

and hence the S/N becomes

$$\begin{aligned}\left(\frac{S}{N}\right)_{\text{pol}}^2 &= \sum_l (2l+1) \frac{\hat{C}_l^{T_\tau}}{C_l^{\text{red}}} \\ &= \sum_l \frac{(2l+1) \hat{C}_l^{T_\tau}}{C_l^{\Delta T_{\text{obs}}} - (C_l^{\Delta T_{\text{obs}}, E_{\text{obs}}})^2 / C_l^{E_{\text{obs}}}}.\end{aligned}\quad (27)$$

Note that we have added the index ‘pol’ to indicate that this is the S/N one obtains when using the polarization data to reduce the variance. Comparing the S/N in equation (27) with the one in equation (13), we see that by including the information contained in the polarization data we reduce the variance in every mode by the term $(C_l^{\Delta T_{\text{obs}}, E_{\text{obs}}})^2 / C_l^{E_{\text{obs}}}$.

Let us now get an impression of how much the variance gets reduced for the different multipoles. To this end, we neglect the detector noise T_{det} and E_{det} , and the foreground noise T_{fg} and E_{fg} ,¹

¹ In reality, galactic E-mode foregrounds E_{fg} are likely to be the limiting factor in the improvement of the detection significance coming from including polarization data. We comment on this at the end of this section.

which allows us to write

$$\begin{aligned} C_l^{\Delta T_{\text{obs}}, E_{\text{obs}}} &\approx C_l^{T_{\text{cmb}}, E_{\text{cmb}}} - C_l^{T_{\tau}, E_{\text{cmb}}} \\ C_l^{\Delta T_{\text{obs}}} &\approx C_l^{T_{\text{cmb}}} - 2C_l^{T_{\text{cmb}}, T_{\tau}} + C_l^{T_{\tau}} \end{aligned} \quad (28)$$

$$C_l^{E_{\text{obs}}} \approx C_l^{E_{\text{cmb}}}. \quad (29)$$

We furthermore neglect the cross-term $C_l^{T_{\tau}, E_{\text{cmb}}}$. For the ISW effect, we have verified numerically that it is negligible. For the kinetic SZ and RS effects, the template itself is so small that we can also certainly neglect $C_l^{T_{\tau}, E_{\text{cmb}}}$. Then, the reduced temperature power spectrum defined in equation (22) becomes

$$C_l^{\text{red}} \approx C_l^{T_{\text{cmb}}} - 2C_l^{T_{\text{cmb}}, T_{\tau}} + C_l^{T_{\tau}} - \frac{(C_l^{T_{\text{cmb}}, E_{\text{cmb}}})^2}{C_l^{E_{\text{cmb}}}}. \quad (30)$$

In Fig. 1, we plot the template-free part of the reduced temperature power spectrum $C_l^{T_{\text{cmb}}} - (C_l^{T_{\text{cmb}}, E_{\text{cmb}}})^2 / C_l^{E_{\text{cmb}}}$ (note that we have not included the template-dependent terms $-2C_l^{T_{\text{cmb}}, T_{\tau}}$ and $C_l^{T_{\tau}}$ in the plot), which gives us an impression of how the variance coming from primordial temperature fluctuations is being reduced by including polarization data. The variance will be further reduced by working conditionally on the signal template T_{τ} , which is encoded in the terms $-2C_l^{T_{\text{cmb}}, T_{\tau}}$ and $C_l^{T_{\tau}}$, and already described in Frommert et al. (2008). We also plot the original CMB power spectrum $C_l^{T_{\text{cmb}}}$ and the difference to the reduced one for comparison. We have assumed a flat Λ CDM model with the parameter values given by Komatsu et al. (2008), table 1 ($\Omega_b h^2 = 0.02265$, $\Omega_{\Lambda} = 0.721$, $h = 0.701$, $n_s = 0.96$, $\tau = 0.084$, $\sigma_8 = 0.817$), and used CMBEASY (www.cmbeasy.org, Doran 2005) for obtaining the respective spectra.

In Fig. 2, we plot a realization of the original temperature map T_{cmb} (top panel), the reduced temperature map T_{red} (middle panel) and the difference of the two, $(C_l^{\Delta T_{\text{obs}}, E_{\text{obs}}} / C_l^{E_{\text{obs}}}) a_{lm}^{E_{\text{obs}}}$, for comparison (bottom panel). The realizations were created using the HEALPIX package (Górski et al. 2005).

Note that all of what we have done works equally well for reducing the E-mode polarization map when trying to detect a secondary signal contained in the polarization data. One has to simply exchange the roles of T and E in the derivation. This was partly already done by Jaffe (2003), who used the information contained

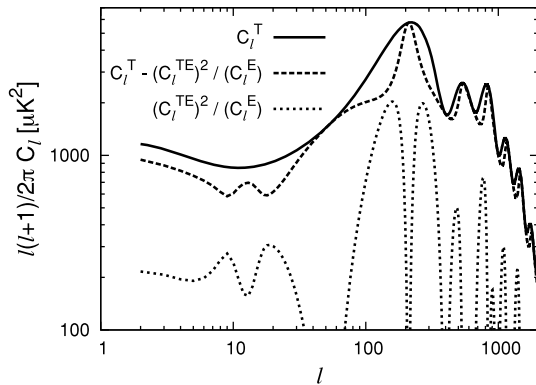


Figure 1. Reduction of the variance in the detection of secondary temperature signals by using the information contained in polarization data. Shown are the CMB temperature power spectrum $C_l^{T_{\text{cmb}}}$ (solid line), and the template-free part of the reduced temperature power spectrum $C_l^{T_{\text{cmb}}} - (C_l^{T_{\text{cmb}}, E_{\text{cmb}}})^2 / C_l^{E_{\text{cmb}}}$ (dashed line), together with the part of the CMB power spectrum coming from the ‘known’ part of the temperature fluctuations which we infer from the polarization map, $(C_l^{T_{\text{cmb}}, E_{\text{cmb}}})^2 / C_l^{E_{\text{cmb}}}$ (dotted line).

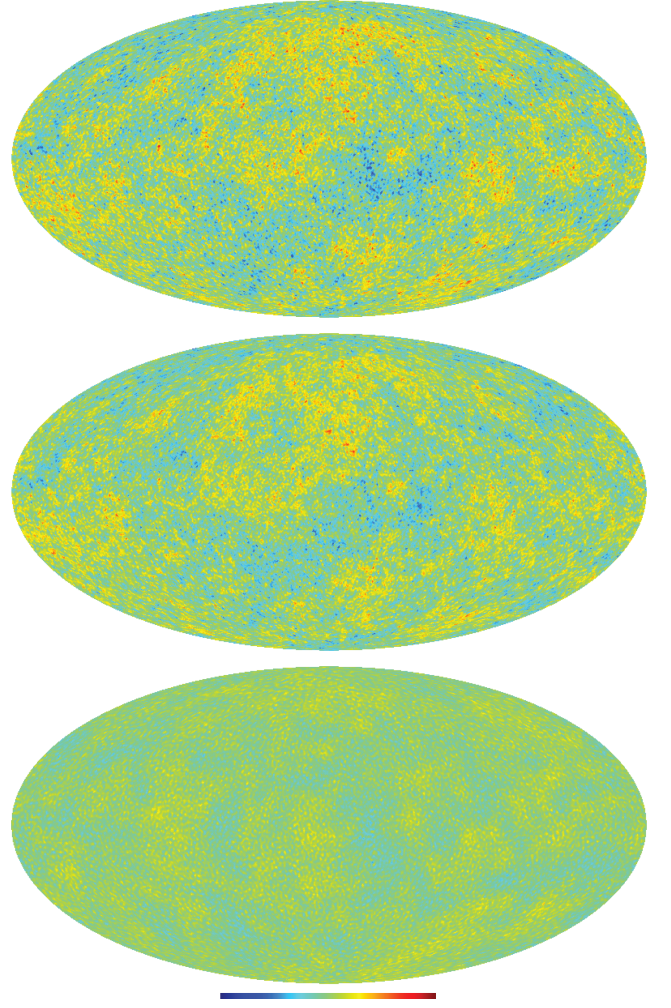


Figure 2. Realization of the original CMB temperature map T_{cmb} (top panel), the reduced temperature map T_{red} (middle panel) and the difference between the two for comparison (bottom panel) in μK . We have chosen the same colour range from -500 to $500 \mu\text{K}$ for all maps.

in the CMB temperature map for predicting a polarization map from it. The equivalent plot to Fig. 1 for this scenario is given in Fig. 3. The likelihood for the case of simultaneously detecting a temperature template T_{τ} and a polarization template E_{τ} is derived in Appendix A.

In practice, the accuracy to which we can measure the E map is limited by galactic foregrounds E_{fg} , the most important of which are synchrotron radiation and dust emission of the Milky Way. Uncertainty in the measured E map makes the reduction of the temperature power spectrum less efficient, because the power contained in the foreground noise, $C_l^{E_{\text{fg}}}$, enhances the observed E-mode power spectrum $C_l^{E_{\text{obs}}} \approx C_l^{E_{\text{cmb}}} + C_l^{E_{\text{fg}}} + C_l^{E_{\text{det}}}$. The prediction of a realistic S/N for our method would require a detailed study of foreground effects, detector noise and scanning strategies, which is beyond the scope of this work.

4 EXAMPLE: THE ISW EFFECT

Let us now apply our method to the ISW effect. That is, our signal template T_{τ} is now an ISW template which we obtain from a Wiener filter reconstruction of the LSS, which can be shown to be optimal for the purpose of ISW detection (Frommert et al.

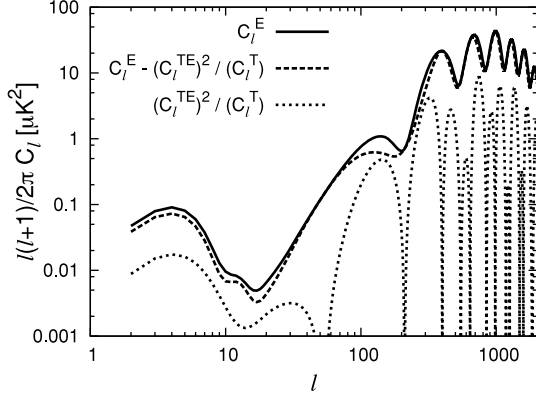


Figure 3. Reduction of the variance in the detection of secondary polarization signals by using the information contained in temperature data. Shown are the CMB E-mode power spectrum $C_l^{E_{\text{cmb}}}$ (solid line), and the template-free part of the reduced E-mode power spectrum $C_l^{E_{\text{cmb}}} - (C_l^{T_{\text{cmb}, E_{\text{cmb}}})^2 / C_l^{T_{\text{cmb}}}$ (dashed line), together with the part of the CMB power spectrum coming from the ‘known’ part of the E-mode fluctuations which we infer from the temperature map, $(C_l^{T_{\text{cmb}, E_{\text{cmb}}})^2 / C_l^{T_{\text{cmb}}}$ (dotted line).

2008). We assume the best-case scenario of having perfect (noiseless) LSS and CMB data. In other words, we neglect the detector noise T_{det} and E_{det} , which is safe on the largest scales, where cosmic variance dominates (Afshordi 2004). We furthermore neglect residual galactic foregrounds T_{fg} and E_{fg} as well as the shot noise in the observed galaxy distribution and assume that we have an ideal galaxy survey that covers the whole sky and goes out to a redshift of at least 2. Then our signal template is exact, $T_{\tau} = T_s \equiv T_{\text{isw}}$, and the residual $(T_{\text{cmb}} - T_{\text{isw}}) \equiv T_{\text{prim}}$ is simply given by the primordial CMB fluctuations, which are created at the surface of last scattering (we have ignored other secondary effects here). We further assume T_{isw} to be uncorrelated with the primordial fluctuations T_{prim} , which is a safe assumption because they are created on very different scales (Boughn et al. 1998). We can then write $C_l^{T_{\text{cmb}, T_{\tau}}} \equiv C_l^{T_{\text{cmb}, T_{\text{isw}}}} = C_l^{T_{\text{isw}}}$.

The S/N for the detection of the ISW signal, equation (27), then reduces to

$$\left(\frac{S}{N}\right)_{\text{pol}}^2 = \sum_l \frac{(2l+1) \hat{C}_l^{T_{\text{isw}}}}{C_l^{T_{\text{prim}}} - (C_l^{T_{\text{prim}, E_{\text{cmb}}})^2 / C_l^{E_{\text{cmb}}}}. \quad (31)$$

As we said before, the S/N depends on the specific LSS realization in our Universe via $\hat{C}_l^{T_{\text{isw}}}$. We can infer its probability distribution from the distribution of T_{isw} by using the central limit theorem for the distribution of $(S/N)^2$ and deriving the distribution for S/N from that (see also Frommert et al. 2008).² We then average the S/N over this probability distribution in order to compare it to the S/N of the standard method and the average S/N of the optimal temperature-only method, both described in Frommert et al. (2008). Recall that the S/N one obtains for the standard method is given by

$$\left(\frac{S}{N}\right)_{\text{st}}^2 = \sum_l \frac{(2l+1) C_l^{T_{\text{isw}}}}{C_l^{T_{\text{prim}}} + C_l^{T_{\text{isw}}}}. \quad (32)$$

The cumulative S/N versus the maximal multipole l_{max} used in the analysis are plotted in Fig. 4. Here, we have assumed the ideal galaxy survey described above. We see that including the polarization data

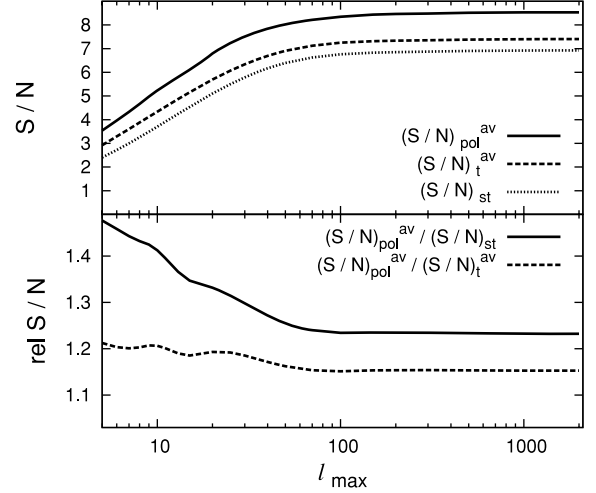


Figure 4. Comparison of the cumulative S/N for $z_{\text{max}} = 2$. Top panel: average S/N ratio of the optimal polarization method $(S/N)_{\text{pol}}^{\text{av}}$ (solid line), of the optimal temperature-only method $(S/N)_{\text{t}}^{\text{av}}$ (dashed line) and S/N of the standard method $(S/N)_{\text{st}}$ (dotted line) versus the maximal multipole considered in the analysis. Bottom panel: ratio of the signal-to-noise of the optimal polarization method with the one of the standard method (solid line) and with the one of the optimal temperature-only method (dashed line).

in the analysis increases the S/N by 16 per cent as compared to the optimal temperature-only method and by 23 per cent as compared to the standard method. Note that we only included the linear ISW effect in Fig. 4. Beyond a multipole of about $l \approx 100$, non-linear effects start to play a crucial role (Cooray 2002), which could change the plot for $l > 100$. However, we see that for the linear ISW effect there is hardly any contribution for such high multipoles.

Let us now look at the enhancement of the S/N for shallower LSS surveys. We use the same approximation as in Frommert et al. (2008), i.e. we introduce a sharp cut-off in redshift and redefine everything beyond that redshift as primordial fluctuations. This introduces a correlation between what we consider the ISW and primordial fluctuations, which we would not have if we had used a proper Wiener filter based template T_{τ} for redefining T_{isw} . However, for getting a rough picture of the redshift dependence, this approximation is good enough.³ We plot the redshift dependence of the S/N of the three methods in Fig. 5. We also plot the ratio of the signal-to-noise of the optimal polarization method with the one of the standard method (solid line) and with the one of the optimal temperature-only method (dashed line). Note that the enhancement of the S/N w.r.t. the optimal temperature-only method is almost constant in redshift. This is quite clear from the fact that we have reduced the *primordial* noise with the polarization data, and neither the primordial noise nor the reduction of the latter depends on redshift. Therefore, the reduction of the noise from including polarization data is always the same, independent of how deep in redshift our survey goes, and the S/N is already significantly enhanced for currently available surveys. For example, for a maximal redshift of $z_{\text{max}} \approx 0.3$, which is the maximal redshift for the Sloan Digital Sky Survey (SDSS) main galaxy sample, we have a better S/N by about 16 per cent as compared to the standard method. The additional enhancement for higher redshifts of our S/N w.r.t. the

² This will provide accurate results for multipoles $l \gg 1$; however, it is a coarse approximation in the regime $l \sim 1$.

³ The ratio of this neglected coupling to the template strength gets large for small z_{max} . Our estimates are therefore less accurate in this regime.

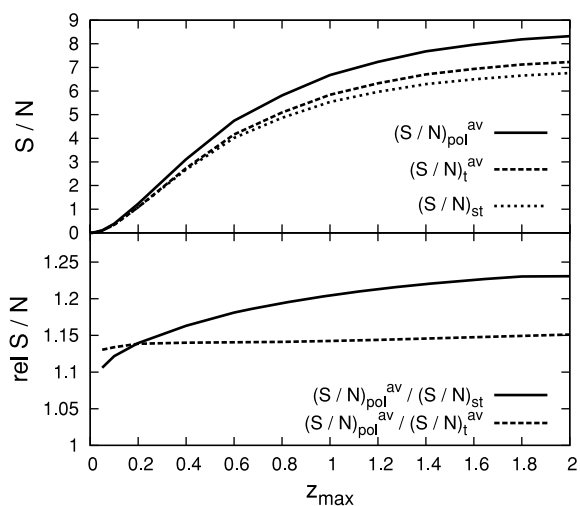


Figure 5. Comparison of the S/N versus the maximal redshift z_{\max} of the galaxy survey. Top panel: average S/N of the optimal polarization method $(S/N)_{\text{pol}}^{\text{av}}$ (solid line), of the optimal temperature-only method $(S/N)_{\text{t}}^{\text{av}}$ (dashed line) and S/N of the standard method $(S/N)_{\text{st}}$ (dotted line). Bottom panel: ratio of the S/N of the optimal polarization method with the one of the standard method (solid line) and with the one of the optimal temperature-only method (dashed line). We see that with polarization data included, the S/N is significantly enhanced even for low redshifts.

standard method comes from working conditionally on the galaxy data, as we have described in detail in Frommert et al. (2008).

5 CONCLUSIONS

The detection of secondary effects on the CMB remains a challenge, because the amplitudes of these effects are much smaller than those of primordial CMB fluctuations. The techniques for detecting such secondary signals are all based on the existing cross-correlation between the LSS and the signal in question. However, in all of these studies, chance correlations of primordial CMB fluctuations with the LSS are the dominant source of noise in the analysis.

We have presented a way of reducing the noise coming from primordial temperature fluctuations by simply subtracting the part of the temperature map which is known from the polarization data. Effectively, only the unknown part of the temperature fluctuations then contributes to the variance of the signal estimate.

As presented here, our method can be generically applied to all secondary effects. However, in this work we have used a Gaussian approximation for the uncertainty in the signal template, which may not be optimal for effects on smaller scales such as the RS effect, the kinetic SZ effect or lensing. We leave the extension of our method to non-Gaussian noise models for future work.

We calculated the achievable reduction in primordial noise for perfect (noiseless) data using the example of the ISW effect, and obtained a S/N of up to 8.5. This corresponds to an enhancement of the S/N by 16 per cent as compared to our optimal temperature-only method, independent of the depth of the LSS survey. In comparison to the standard method, the S/N is enhanced by 23 per cent for a full-sky galaxy survey which goes out to a redshift of at least 2. When using the SDSS main galaxy sample, which has a maximal redshift of about $z_{\max} \approx 0.3$, our S/N is still enhanced by about 16 per cent as compared to the standard method.

The variance reduction achieved with this method will significantly improve the detection of all kinds of secondary effects on the CMB, where a spatial template constructed from non-CMB data can

be created. This stresses the importance of accurate measurements of primordial polarization fluctuations even for non-primordial signal detection and analysis. The upcoming Planck Surveyor Mission, as well as more future experiments like PolarBear⁴ or CMBPol,⁵ will allow us to benefit from polarization for the detection of secondary CMB signals in the way presented in this work.

ACKNOWLEDGMENTS

The authors would like to thank Martin Reinecke and André Waelkens for their extensive help with HEALPIX. We would also like to thank Simon D. M. White, Cheng Li and Thomas Riller for useful discussions and comments. We acknowledge the use of the HEALPIX package and CMBEASY.

REFERENCES

- Afshordi N., 2004, *Phys. Rev. D*, 70, 083536
 Baumann D. et al., 2008, preprint (arXiv:0811.3919B)
 Boughn S., Crittenden R., 2004, *Nat*, 427, 45
 Boughn S. P., Crittenden R. G., Turok N. G., 1998, *New Astron.*, 3, 275
 Cooray A., 2002, *Phys. Rev. D*, 65, 083518
 Cooray A., Melchiorri A., 2006, *J. Cosmol. Astropart. Phys.*, 1, 18
 Crittenden R., 2006, <http://www-astro-theory.fnal.gov/Conferences/ECcmbC/PresentationFiles/RobertCrittenden.ppt>, <http://www-astro-theory.fnal.gov/Conferences/ECcmbC/ECcmbCagenda.html>
 Doran M., 2005, *J. Cosmol. Astropart. Phys.*, 10, 11
 Enßlin T. A., Frommert M., Kitaura F. S., 2008, *Phys. Rev. D*, submitted (astro-ph/0806.3474)
 Frommert M., Enßlin T. A., Kitaura F. S., 2008, *MNRAS*, 391, 1315
 Giannantonio T., Scranton R., Crittenden R. G., Nichol R. C., Boughn S. P., Myers A. D., Richards G. T., 2008, *Phys. Rev. D*, 77, 123520
 Górski K. M., Hivon E., Banday A. J., Wandelt B. D., Hansen F. K., Reinecke M., Bartelmann M., 2005, *ApJ*, 622, 759
 Granett B. R., Neyrinck M. C., Szapudi I., 2008, preprint (astro-ph/0805.2974)
 Haehnelt M. G., Tegmark M., 1996, *MNRAS*, 279, 545
 Hernández-Monteagudo C., 2008, *A&A*, 490, 15
 Ho S., Hirata C., Padmanabhan N., Seljak U., Bahcall N., 2008, *Phys. Rev. D*, 78, 043519
 Jaffe A. H., 2003, *New Astron. Rev.*, 47, 1001
 Komatsu E. et al., 2008, *ApJS*, 180, 330
 Lewis A., Challinor A., 2006, *Phys. Rep.*, 429, 1
 Maturi M., Dolag K., Waelkens A., Springel V., Enßlin T., 2007a, *A&A*, 476, 83
 Maturi M., Enßlin T., Hernández-Monteagudo C., Rubiño-Martín J. A., 2007b, *A&A*, 467, 411
 Rassat A., Land K., Lahav O., Abdalla F. B., 2007, *MNRAS*, 377, 1085
 Rees M. J., Sciama D. W., 1968, *Nat*, 217, 511
 Sachs R. K., Wolfe A. M., 1967, *ApJ*, 147, 73
 Schäfer B. M., Pfrommer C., Hell R. M., Bartelmann M., 2006, *MNRAS*, 370, 1713
 Sunyaev R. A., Zeldovich Y. B., 1972, *Comments Astrophys. Space Phys.*, 4, 173
 Sunyaev R. A., Zeldovich Y. B., 1980, *ARA&A*, 18, 537
 Tauber J. A., 2000, *Astrophys. Lett. Commun.*, 37, 145
 Waelkens A., Maturi M., Enßlin T., 2008, *MNRAS*, 383, 1425
 Zaldarriaga M., 1997, *Phys. Rev. D*, 55, 1822
 Zhang P., 2006, *ApJ*, 647, 55

⁴ <http://bolo.berkeley.edu/polarbear/index.html>

⁵ Baumann et al. (2008); <http://cmbpol.uchicago.edu>.

APPENDIX A: PROOF OF THE FACTORIZATION OF THE LIKELIHOOD

We now explicitly prove the factorization of the likelihood in equation (21) into a reduced temperature part and a polarization part, as given in equation (23). We will do this for the more general case that we not only have a signal template T_τ for the temperature part but also a non-zero template E_τ for the polarization part. In this case, the covariance matrix is

$$\tilde{\mathbf{C}}(l) = \begin{pmatrix} C_l^{\Delta T_{\text{obs}}} & C_l^{\Delta T_{\text{obs}}, \Delta E_{\text{obs}}} \\ C_l^{\Delta T_{\text{obs}}, \Delta E_{\text{obs}}} & C_l^{\Delta E_{\text{obs}}} \end{pmatrix}, \quad (\text{A1})$$

instead of the simplified one given in equation (20). Here, ΔE_{obs} is defined as $\Delta E_{\text{obs}} \equiv E_{\text{obs}} - E_\tau$. The inverse of the covariance matrix is given by

$$\tilde{\mathbf{C}}(l)^{-1} = \frac{1}{C_l^{\Delta T_{\text{obs}}} C_l^{\Delta E_{\text{obs}}} - \left(C_l^{\Delta T_{\text{obs}}, \Delta E_{\text{obs}}}\right)^2} \times \begin{pmatrix} C_l^{\Delta E_{\text{obs}}} & -C_l^{\Delta T_{\text{obs}}, \Delta E_{\text{obs}}} \\ -C_l^{\Delta T_{\text{obs}}, \Delta E_{\text{obs}}} & C_l^{\Delta T_{\text{obs}}} \end{pmatrix}. \quad (\text{A2})$$

We first rewrite the exponent of $\mathcal{G}[a_{lm}^d - a_{lm}^\tau, \tilde{\mathbf{C}}(l)]$ in equation (21) by inserting the inverse of $\tilde{\mathbf{C}}(l)$:

$$\begin{aligned} & \left(a_{lm}^{T_{\text{obs}}} - a_{lm}^{T_\tau}, a_{lm}^{E_{\text{obs}}} - a_{lm}^{E_\tau}\right) \tilde{\mathbf{C}}(l)^{-1} \left(a_{lm}^{T_{\text{obs}}} - a_{lm}^{T_\tau}, a_{lm}^{E_{\text{obs}}} - a_{lm}^{E_\tau}\right)^\dagger \\ &= \left[\left| a_{lm}^{\Delta T_{\text{obs}}} \right|^2 - 2 \left(C_l^{\Delta T_{\text{obs}}, \Delta E_{\text{obs}}} / C_l^{\Delta E_{\text{obs}}} \right) \text{Re} \left(a_{lm}^{\Delta E_{\text{obs}}} a_{lm}^{\Delta T_{\text{obs}}} \right) \right. \\ & \quad \left. + \left(C_l^{\Delta T_{\text{obs}}} / C_l^{\Delta E_{\text{obs}}} \right) \left| a_{lm}^{\Delta E_{\text{obs}}} \right|^2 \right] \\ & \quad / \left[C_l^{\Delta T_{\text{obs}}} - \left(C_l^{\Delta T_{\text{obs}}, \Delta E_{\text{obs}}} \right)^2 / C_l^{\Delta E_{\text{obs}}} \right] \end{aligned}$$

$$\begin{aligned} &= \frac{\left| a_{lm}^{\Delta T_{\text{obs}}} - \left(C_l^{\Delta T_{\text{obs}}, \Delta E_{\text{obs}}} / C_l^{\Delta E_{\text{obs}}} \right) a_{lm}^{\Delta E_{\text{obs}}} \right|^2}{C_l^{\Delta T_{\text{obs}}} - \left(C_l^{\Delta T_{\text{obs}}, \Delta E_{\text{obs}}} \right)^2 / C_l^{\Delta E_{\text{obs}}}} \\ & \quad + \frac{\left| a_{lm}^{\Delta E_{\text{obs}}} \right|^2}{C_l^{\Delta E_{\text{obs}}}} \\ & \equiv \frac{\left| a_{lm}^{T_{\text{red}}} - a_{lm}^{T_\tau} \right|^2}{C_l^{\text{red}}} + \frac{\left| a_{lm}^{E_{\text{obs}}} - a_{lm}^{E_\tau} \right|^2}{C_l^{\Delta E_{\text{obs}}}}, \quad (\text{A3}) \end{aligned}$$

where we have completed the square in the second last step and used a generalized definition of the reduced temperature map and power spectrum, which we had introduced in equation (22), in the last step. Similarly, we can decompose the determinant of $\tilde{\mathbf{C}}(l)$:

$$\begin{aligned} |\tilde{\mathbf{C}}(l)| &= C_l^{\Delta T_{\text{obs}}} C_l^{\Delta E_{\text{obs}}} - \left(C_l^{\Delta T_{\text{obs}}, \Delta E_{\text{obs}}} \right)^2 \\ &\equiv C_l^{\text{red}} C_l^{\Delta E_{\text{obs}}}. \end{aligned}$$

Inserting equations (A3) and (A4) into $\mathcal{G}[a_{lm}^d - a_{lm}^\tau, \tilde{\mathbf{C}}(l)]$ allows us to write

$$\begin{aligned} \mathcal{G}[a_{lm}^d - a_{lm}^\tau, \tilde{\mathbf{C}}(l)] &= \mathcal{G}(a_{lm}^{T_{\text{red}}} - a_{lm}^{T_\tau}, C_l^{\text{red}}) \\ & \quad \times \mathcal{G}(a_{lm}^{E_{\text{obs}}} - a_{lm}^{E_\tau}, C_l^{\Delta E_{\text{obs}}}). \quad (\text{A4}) \end{aligned}$$

In the case of the polarization template E_τ being zero, this expression reduces to the one in equation (23).

This paper has been typeset from a $\text{\TeX}/\text{\LaTeX}$ file prepared by the author.